

Competition between the structural phase transition and superconductivity in $\text{Ir}_{1-x}\text{Pt}_x\text{Te}_2$ as revealed by pressure effects

A. Kiswandhi,^{1,2} J. S. Brooks,^{1,2} H. B. Cao,³ J. Q. Yan,^{4,5} D. Mandrus,^{4,5} Z. Jiang,⁶ and H. D. Zhou^{1,7,*}

¹National High Magnetic Field Laboratory, Florida State University, Tallahassee, Florida 32306-4005, USA

²Department of Physics, Florida State University, Tallahassee, Florida 32306-3016, USA

³Quantum Condensed Matter Division, Oak Ridge National Laboratory, Oak Ridge, Tennessee 37831, USA

⁴Materials Science and Technology Division, Oak Ridge National Laboratory, Oak Ridge, Tennessee 37831, USA

⁵Department of Materials and Engineering, University of Tennessee, Knoxville, Tennessee 37996, USA

⁶School of Physics, Georgia Institute of Technology, Atlanta, Georgia 30332, USA

⁷Department of Physics and Astronomy, University of Tennessee, Knoxville, Tennessee 37996-1200, USA

(Received 27 December 2012; revised manuscript received 6 March 2013; published 18 March 2013)

Pressure-dependent transport measurements of $\text{Ir}_{1-x}\text{Pt}_x\text{Te}_2$ are reported. With increasing pressure, the structural phase transition at high temperatures is enhanced while its superconducting transition at low temperatures is suppressed. These pressure effects make $\text{Ir}_{1-x}\text{Pt}_x\text{Te}_2$ distinct from other studied TX_2 systems exhibiting a charge density wave (CDW) state, in which pressure usually suppresses the CDW state and enhances the superconducting state. The results reveal that the emergence of superconductivity competes with the stabilization of the low-temperature monoclinic phase in $\text{Ir}_{1-x}\text{Pt}_x\text{Te}_2$.

DOI: [10.1103/PhysRevB.87.121107](https://doi.org/10.1103/PhysRevB.87.121107)

PACS number(s): 74.62.Fj, 74.25.Dw, 74.70.Ad

One of the fundamental interests in the physics of transition-metal dichalcogenides (TX_2 , $T = \text{Ti, Ta, or Nb}$, $X = \text{S, Se, or Te}$) with $1T$ and $2H$ structures is the competition between two very different phenomena: a charge density wave (CDW) state and superconductivity.^{1–3} Although the studies on TX_2 have been ongoing for almost half a century, the microscopic origin of the CDW state is not yet fully understood. On the other hand, studies of TX_2 systems have revealed interesting physical behavior.^{4–8}

Recently another member of the TX_2 family with a $5d$ transition metal, IrTe_2 , has received a lot of attention due to its properties: (I) At room temperature, the $1T$ - IrTe_2 crystallizes in a trigonal structure with the edge-sharing IrTe_6 octahedra, forming layers stacked along the c axis [Fig. 1(a)], with the Ir ions forming equilateral triangular lattices in the ab plane [Fig. 1(b)]. By decreasing temperature, at around 250 K shorter Ir-Ir bonds form and the structure transforms into a monoclinic structure [Figs. 1(c), 1(d)]. This transition is accompanied with a jump in resistivity and a decrease in susceptibility.⁹ This phenomenon is similar to that of the CDW state in other TX_2 systems. However the early NMR studies did not support the CDW transition scenario in IrTe_2 .¹⁰ Recent electron diffraction¹¹ and photoemission studies¹² both suggested that the Ir t_{2g} orbitals could contribute in the transition. Therefore, the exact origin of this transition is still unclear. (II) Due to its large atomic number, IrTe_2 is expected to show a strong spin-orbital (SO) coupling, which has been shown to result in unique quantum states in other materials, e.g., the $J_{\text{eff}} = 1/2$ Mott insulator in Sr_2IrO_4 ¹³ and topological insulators.^{14–16} (III) More interestingly, recent studies show that a small percentage of Pd or Pt doping induces superconductivity at temperatures below 4 K in the parent compound.^{11,17} However, it is still unclear whether the origin of the superconducting transition is similar to that of the other TX_2 systems with a CDW state.

In this Rapid Communication, we use hydrostatic pressure as a tool to influence the transitions in $\text{Ir}_{1-x}\text{Pt}_x\text{Te}_2$. Transport

measurements performed at different pressures clearly show that the structural phase transition temperature increases while the superconducting transition temperature decreases with increasing pressure. These pressure effects make IrTe_2 distinct from most other TX_2 systems in which pressure usually suppresses the CDW states while enhancing the superconductivity. The results show that $\text{Ir}_{1-x}\text{Pt}_x\text{Te}_2$ is a unique system due to the competition between the structural and superconducting transitions.

Single crystals of IrTe_2 and $\text{Ir}_{0.95}\text{Pt}_{0.05}\text{Te}_2$ were grown using a self-flux technique as recently reported.¹⁸ The polycrystalline samples $\text{Ir}_{0.98}\text{Pt}_{0.02}\text{Te}_2$ and $\text{Ir}_{0.97}\text{Pt}_{0.03}\text{Te}_2$ were prepared by standard solid-state reaction. To avoid the grain boundary effect in transport measurements, the dense and hard pellets of the polycrystalline samples were prepared by a cold-press technique.¹⁹ The transport measurements were performed using a four-probe technique and the hydrostatic pressure was generated by using Daphne oil 7373 as a pressure medium in a standard piston cylinder clamp cell. At low temperature, the pressure generated by the Daphne oil 7373 is known to decrease by approximately 1.5 kbar.²⁰ Any pressure mentioned in this communication will be the pressure as measured at room temperature. Single-crystal neutron diffraction measurements were performed at the HB-3A four-circle diffractometer at the High Flux Isotope Reactor at the Oak Ridge National Laboratory.

The structural phase transition temperature was determined from the transport measurement since the transition is accompanied with an increase in the resistivity (ρ). Here, T_s is defined as the minimum of $d\rho/dT$. At the ambient pressure T_s was found to be 264 K and 272 K for IrTe_2 during the cool-down and warm-up processes, respectively [Fig. 2(a)], which is consistent with a previous report.¹⁸ With increasing pressure, T_s increases linearly with $dT_s/dP = 4.393$ K/kbar [Fig. 2(b)]. Here dT_s/dP is the average of dT_s/dP during the cool-down and warm-up processes, as the values are very similar. The transport measurement shows a thermal

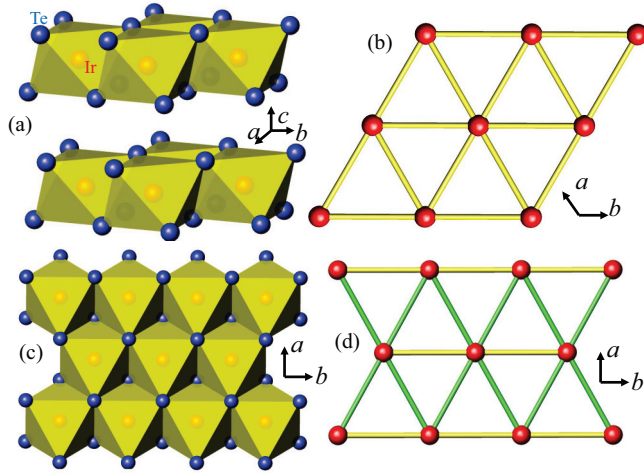


FIG. 1. (Color online) (a) The lattice structure of IrTe₂ in the trigonal phase at $T > T_s$ showing (b) the equilateral triangular lattice of Ir atoms in the ab plane. (c) The lattice structure of IrTe₂ in the monoclinic phase at $T < T_s$ showing (d) the isosceles triangular lattice of Ir atoms in the ab plane. In (d) the two green lines represent the short Ir-Ir bonds.

hysteresis, characteristic of a first-order transition. IrTe₂ shows no superconductivity down to 1.3 K at all measured pressures (not shown).

In Ir_{1-x}Pt_xTe₂ samples at ambient pressure, T_s is suppressed to lower temperatures, and superconductivity appears below 4 K with increasing Pt doping (Fig. 3), which is consistent

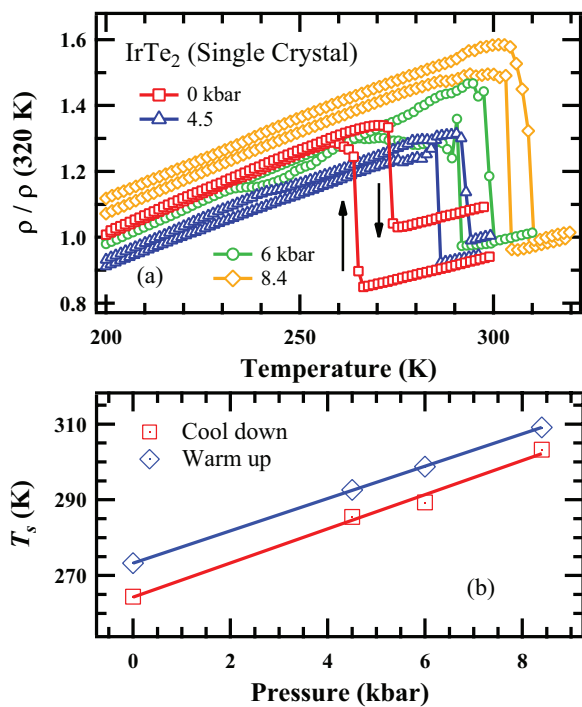


FIG. 2. (Color online) (a) Temperature dependence of resistivity of IrTe₂ at various pressures showing a clockwise thermal hysteresis around the structural transition. For $P < 8.4$ kbar, $\rho(320 \text{ K})$ was obtained by extrapolating the linear part at $T > T_s$. (b) Pressure dependence of T_s for cool-down and warm-up runs.

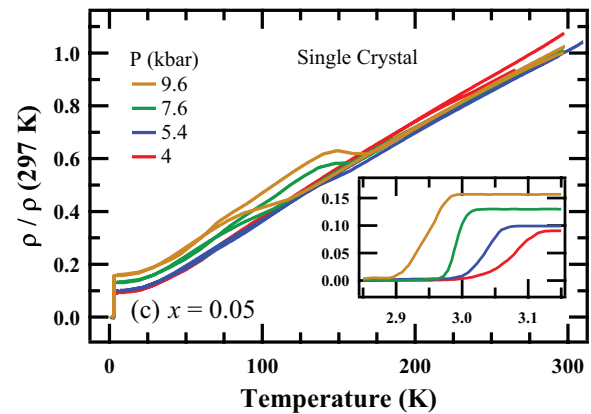
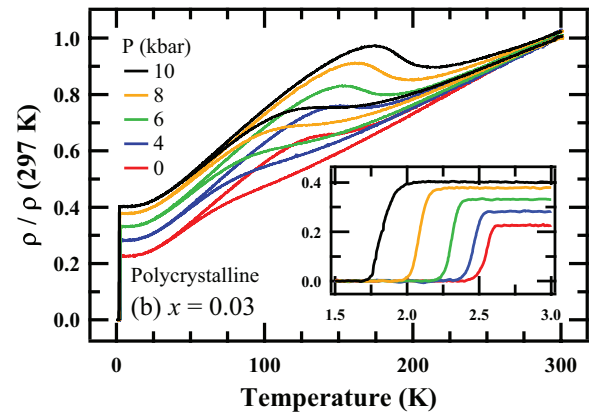
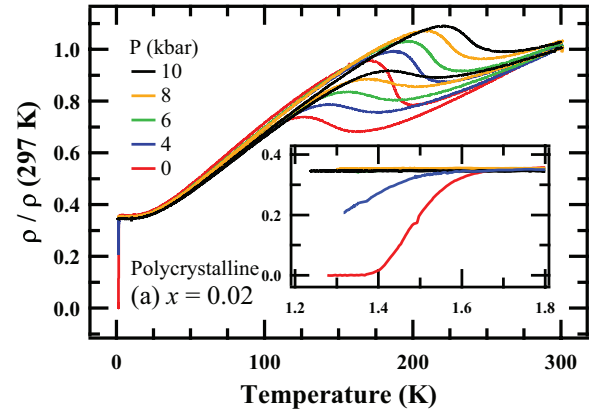


FIG. 3. (Color online) Temperature dependence of normalized resistivity for Ir_{1-x}Pt_xTe₂ at various pressures. Polycrystalline samples with (a) $x = 0.02$ and (b) $x = 0.03$. (c) Single crystal with $x = 0.05$. The insets show the superconducting transition part of each corresponding figure.

with the reported data.¹⁷ For $x = 0.02$ and 0.03 , T_s increases linearly with increasing pressure and the rates are 5.235 K/kbar and 4.098 K/kbar, respectively. For $x = 0.03$, the superconducting transition temperature T_{SC} shifts toward lower temperatures with increasing pressure with a rate $dT_{SC}/dP = -0.09$ K/kbar [inset of Fig. 3(b)]. For $x = 0.02$, the superconducting transition is not yet complete at $P \geq 4$ kbar at the lowest accessible temperature. The single crystal $x = 0.05$ shows no detectable anomaly or hysteresis as apparent as in $x \leq 0.03$, at $P \leq 5.4$ kbar. Similar to other samples, its T_{SC} decreases with increasing pressure with a rate of -0.025 K/kbar. However, at 7.6 kbar, the thermal hysteresis

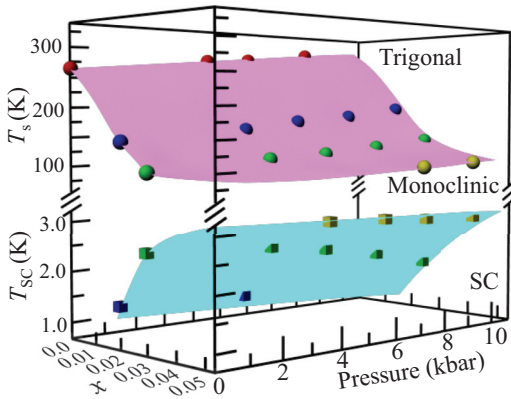


FIG. 4. (Color online) The phase diagram of $\text{Ir}_{1-x}\text{Pt}_x\text{Te}_2$. The spheres and the cubes represent the experimental values of T_s and T_{SC} , respectively. Here the T_s values are obtained from the cool-down process. The surfaces are the schematic phase boundaries separating the trigonal (metallic), monoclinic (metallic), and superconducting phases.

reappeared at $T_s = 96.5$ K and 151.6 K during cool-down and warm-up, respectively, for $x = 0.05$. At 9.6 kbar T_s increases to 100.7 K and 156 K, respectively.

For $x = 0, 0.02$, and 0.03 , it is clear that the resistivity jump is related to the structural phase transition. The increase of T_s for these three samples with increasing pressure indicates that the low-temperature monoclinic phase is stabilized by pressure. The Pt doping completely suppresses the structural phase transition for $x = 0.05$ at low pressures and as a result no resistivity jump or hysteresis was observed. The reappearance of the resistivity anomaly for $x = 0.05$ at high pressures, with features similar to that of the low-doping samples, clearly indicates that the structural phase transition is recovered in this sample at high pressures above 7.6 kbar. It is also noticed that for $x = 0.02$, the resistivity increases around T_s with increasing pressure; and for $x = 0.03$ and 0.05 , the resistivity increases for the whole temperature region below T_s with increasing pressure.

The overall behavior of the system revealed by pressure effects is summarized in Fig. 4. Using pressure as a controlled parameter, the structural transition temperature of $\text{Ir}_{1-x}\text{Pt}_x\text{Te}_2$ is enhanced in temperatures and the superconducting transition temperature is reduced. For $x = 0.05$, the structural phase transition, suppressed by Pt doping, is recovered by high pressure. The competition between the structural phase transition and superconductivity is clearly revealed.

In some of the TX_2 systems, such as 2H-TaSe_2 , 2H-TaS_2 , and 2H-NbSe_2 , the CDW transition coexists with the superconductivity.¹⁻⁴ On the other hand, in 1T-TiSe_2 ^{5,6} and 1T-TaS_2 ,^{7,21} the superconductivity can be achieved by doping or pressure. Generally, for TX_2 systems, the doping mainly shifts the chemical potential into the conduction band due to donor electrons and the pressure mainly increases $N(E_F)$ by suppressing the CDW state and restoring the Fermi surface to the undistorted state. Therefore, both doping and pressure have similar effects on TX_2 systems: suppressing the CDW transition and enhancing the superconductivity.^{5-7,22-26} The pressure studies on TX_2 without introducing any degree of

internal disorder by doping clearly demonstrate the competition between the CDW state and superconductivity.

It is apparent that the pressure effects on 1T-IrTe_2 and related Pt-doped samples are different from those on other TX_2 systems. The reported powder x-ray diffraction studies on IrTe_2 show that the high-temperature transition is of a structural nature from a trigonal to a monoclinic structure with space group $C2/m$. The transition causes the Ir-Ir distance to contract along the b axis, establishing an Ir-Ir bond. On the other hand, the distance between the IrTe_6 layers along the c axis expands.^{9,17} Based on the similarity of the structural distortion between IrTe_2 and another triangular lattice material NaTiO_2 with $\text{Ti}^{3+} t_{2g}$ orbital ordering,^{27,28} Pyon *et al.*¹⁷ proposed that the structural phase transition in IrTe_2 could be induced by the ordering of the Ir $5d t_{2g}$ orbitals. The most recent photoemission results also suggest an orbitally induced Peierls effect in IrTe_2 .¹² Moreover, Yang *et al.*¹¹ proposed a charge-orbital density wave scenario for IrTe_2 , based on the fact that the structural phase transition is accompanied by the emergence of superlattice peaks. Although the exact origin of the structural phase transition for IrTe_2 is unclear, all of the studies indicate that the transition is not exactly CDW based as shown by other TX_2 systems but more likely related to orbital ordering. Another fact is that no electronic phase transition is induced by the structural phase transition in IrTe_2 , but only a resistivity jump in a generally metallic behavior over the entire temperature region. Therefore, in IrTe_2 the structural distortion is the main phenomenon leading to the observed transport behavior. For other TX_2 systems with a CDW transition, the lattice deformation is usually regarded as being caused by electronic ordering. This fundamental difference could be the primary reason for the different pressure effects between IrTe_2 and other TX_2 systems.

Recently, single-crystal x-ray and neutron diffraction measurements on an as-prepared IrTe_2 sample were also performed to revisit its structure.²⁹ The results confirmed that the low-temperature phase is a monoclinic phase, but with the contraction of two of the three nearest Ir-Ir bonds instead of only one as in the previously reported powder x-ray diffraction studies. An orbital ordering transition of the Ir sites is proposed to account for these two bond contractions and the resulting structural phase transition with the IrTe_6 octahedra distortion. More importantly, the volume shows a 1.0% decrease below the structural phase transition.²⁹ Therefore, when the applied pressure contracts the IrTe_2 volume, the low-temperature, smaller volume monoclinic phase is stabilized, resulting in an increase in T_s . The stabilization of the low-temperature phase by pressure is also shown by the increase of the resistivity below T_s with increasing pressure for Pt-doped samples, since the low-temperature monoclinic phase favors higher resistivity due to the resistivity jump around T_s . The pressure effects on IrTe_2 are analogous to those of spinel CuIr_2S_4 . In CuIr_2S_4 , the structural transition occurs from cubic to tetragonal with a volume contraction of 0.7%³⁰ due to the orbitally induced Peierls state below T_s .³¹ The transition is accompanied by a metal-insulator transition due to the charge ordering of Ir^{3+} - Ir^{4+} electrons.³² In contrast to most systems exhibiting metal-insulator transitions, high pressure stabilizes the low-temperature insulating phase for CuIr_2S_4 , leading to an increase in T_s and resistivity below T_s .³³ While the dT_s/dP

for CuIr_2S_4 was found to be about 2.8 K/kbar, smaller than that of $\text{Ir}_{1-x}\text{Pt}_x\text{Te}_2$, which is 4.0 ~ 5.0 K/kbar, the similarity of the phenomenon could be useful to understand the exact origin of the structural phase transition in IrTe_2 and more studies are needed.

In the Pt-doped samples, while the monoclinic phase is stabilized by pressure, the superconductivity is suppressed simultaneously. In the case of $x = 0.05$, the structural phase transition is recovered with high pressures at 7.6 kbar. These pressure effects clearly show the competition between the structural phase transition and superconductivity: The stabilization of the monoclinic phase suppresses the superconductivity. On the other hand, with increasing Pt doping, T_s is suppressed and superconductivity emerges. Pyon *et al.* have already pointed out that the breaking of Ir-Ir bonds in the monoclinic phase by Pt doping results in the appearance of superconductivity. The pressure and Pt doping affect the transitions in the opposite way. However, both effects consistently show that the structural fluctuations related to Ir-Ir bond formation in $\text{Ir}_{1-x}\text{Pt}_x\text{Te}_2$ are critical for the emergence of superconductivity. While the Ir-Ir bond in the monoclinic

phase is stabilized by pressure (is broken by doping), the superconductivity is suppressed (is induced by doping).

In conclusion, the transport measurement at different pressures on $\text{Ir}_{1-x}\text{Pt}_x\text{Te}_2$ clearly revealed the competition between the structural phase transition at high temperatures and the superconductivity at low temperatures. This makes $\text{Ir}_{1-x}\text{Pt}_x\text{Te}_2$ unique compared with most TX_2 systems that have been studied, in which the competition is between two phases: the CDW state and superconductivity. $\text{Ir}_{1-x}\text{Pt}_x\text{Te}_2$ provides a unique case to study the close relationship between structural fluctuations and superconductivity.

The authors would like to thank Stanley Tozer, Vaughan Williams, Daniel McIntosh, Robert Schwartz, and David Graf for technical assistance concerning the pressure cell used in this work. This work is supported by NSF-DMR-0654118 and the State of Florida. A.K. is supported in part by NSF-DMR-1005293. Work at ORNL was supported by the US Department of Energy, Office of Basic Energy Sciences, the Scientific User Facilities Division (H.B.C.) and the Materials Science and Engineering Division (J.Q.Y. and D.G.M.).

*hzhou10@utk.edu

¹R. L. Withers and J. A. Wilson, *J. Phys. C* **19**, 4809 (1986).

²J. A. Wilson and A. D. Yoffe, *Adv. Phys.* **18**, 193 (1969).

³J. A. Wilson, F. J. DiSalvo, and S. Mahajan, *Adv. Phys.* **24**, 117 (1975).

⁴A. H. Castro Neto, *Phys. Rev. Lett.* **86**, 4382 (2001).

⁵A. F. Kusmartseva, B. Sipoš, H. Berger, L. Forró, and E. Tutiš, *Phys. Rev. Lett.* **103**, 236401 (2009).

⁶E. Morosan, H. W. Zandbergen, B. S. Dennis, J. W. G. Bos, Y. Onose, T. Klimczuk, A. P. Ramirez, N. P. Ong, and R. J. Cava, *Nat. Phys.* **2**, 544 (2006).

⁷B. Sipoš, A. F. Kusmartseva, A. Akrap, H. Berger, L. Forró, and E. Tutiš, *Nat. Mater.* **7**, 960 (2008).

⁸T. Valla, A. V. Fedorov, P. D. Johnson, P.-A. Glans, C. McGuinness, K. E. Smith, E. Y. Andrei, and H. Berger, *Phys. Rev. Lett.* **92**, 086401 (2004).

⁹N. Matsumoto, K. Taniguchi, R. Endoh, H. Takano, and S. Nagata, *J. Low. Temp. Phys.* **117**, 1129 (1999).

¹⁰K. Mizuno, K. Magishi, Y. Shinonome, T. Saito, K. Koyama, N. Matsumoto, and S. Nagata, *Physica B* **312-313**, 818 (2002).

¹¹J. J. Yang, Y. J. Choi, Y. S. Oh, A. Hogan, Y. Horibe, K. Kim, B. I. Min, and S.-W. Cheong, *Phys. Rev. Lett.* **108**, 116402 (2012).

¹²D. Ootsuki, Y. Wakisaka, S. Pyon, K. Kudo, M. Nohara, M. Arita, H. Anzai, H. Namatame, M. Taniguchi, N. L. Saini, and T. Mizokawa, *Phys. Rev. B* **86**, 014519 (2012).

¹³B. J. Kim, H. Jin, S. J. Moon, J.-Y. Kim, B.-G. Park, C. S. Leem, J. Yu, T. W. Noh, C. Kim, S.-J. Oh, J.-H. Park, V. Durairaj, G. Cao, and E. Rotenberg, *Phys. Rev. Lett.* **101**, 076402 (2008).

¹⁴Y. Xia, D. Qian, D. Hsieh, L. Wray, A. Pal, H. Lin, A. Bansil, D. Grauer, Y. S. Hor, R. J. Cava, and M. Z. Hasan, *Nat. Phys.* **5**, 398 (2009).

¹⁵M. Z. Hasan and C. L. Kane, *Rev. Mod. Phys.* **82**, 3045 (2010).

¹⁶X.-L. Qi and S.-C. Zhang, *Rev. Mod. Phys.* **83**, 1057 (2011).

¹⁷S. Pyon, K. Kudo, and M. Nohara, *J. Phys. Soc. Jpn.* **81**, 053701 (2012).

¹⁸A. F. Fang, G. Xu, T. Dong, P. Zheng, and N. L. Wang, *Sci. Rep.* **3**, 1153 (2013).

¹⁹J.-S. Zhou, J. B. Goodenough, and B. Dabrowski, *Phys. Rev. B* **67**, 020404(R) (2003).

²⁰K. Murata, H. Yoshino, H. O. Yadav, Y. Honda, and N. Shirakawa, *Rev. Sci. Instrum.* **68**, 2490 (1997).

²¹L. Fang, Y. Wang, P. Y. Zou, L. Tang, Z. Xu, H. Chen, C. Dong, L. Shan, and H. H. Wen, *Phys. Rev. B* **72**, 014534 (2005).

²²T. F. Smith, L. E. DeLong, A. R. Moodenbaugh, T. H. Geballe, and R. E. Schwall, *J. Phys. C* **5**, L230 (1972).

²³A. H. Thompson, F. R. Gamble, and R. F. Koehler, *Phys. Rev. B* **5**, 2811 (1972).

²⁴P. Molinié, D. Jérôme, and A. J. Grant, *Philos. Mag.* **30**, 1091 (1974).

²⁵C. Berthier, P. Molinié, and D. Jérôme, *Solid State Commun.* **18**, 1393 (1976).

²⁶R. H. Friend and D. Jérôme, *J. Phys. C* **12**, 1441 (1979).

²⁷K. Takeda, K. Miyake, K. Takeda, and K. Hirakawa, *J. Phys. Soc. Jpn.* **61**, 2156 (1992).

²⁸S. J. Clarke, A. J. Fowkes, A. Harrison, R. M. Ibberson, and M. J. Rosseinsky, *Chem. Mater.* **10**, 372 (1998).

²⁹H. B. Cao, B. C. Chakoumakos, J. Q. Yan, H. D. Zhou, R. Custelcean, and D. Mandrus, arXiv:1302.5369.

³⁰T. Furubayashi, T. Matsumoto, T. Hagino, and S. Nagata, *J. Phys. Soc. Jpn.* **63**, 3333 (1994).

³¹D. I. Khomskii and T. Mizokawa, *Phys. Rev. Lett.* **94**, 156402 (2005).

³²P. G. Radaelli, Y. Horibe, M. J. Guttman, H. Ishibashi, C. H. Chen, R. M. Ibberson, Y. Koyama, Y.-S. Hor, V. Kiryukhin, and S.-W. Cheong, *Nature (London)* **416**, 155 (2002).

³³G. Oomi, T. Kagayama, I. Yoshida, T. Hagino, and S. Nagata, *J. Magn. Magn. Mater.* **140-144**, 157 (1995).